Journal of Molecular Catalysis A: Chemical 334 (2011) 29–34

Journal of Molecular Catalysis A: Chemical

journal homepage: www.elsevier.com/locate/molcata

Chemicals from ethanol – The dehydrogenative route of the ethyl acetate one-pot synthesis

Priscila C. Zonetti, Johnatan Celnik, Sonia Letichevsky, Alexandre B. Gaspar, Lucia G. Appel*

Instituto Nacional de Tecnologia/MCT, Av. Venezuela 82/518, Rio de Janeiro 21081-312, Brazil

ARTICLE INFO

Article history:
Received 9 June 2010
Received in revised form 20 October 2010
Accepted 25 October 2010
Available online 30 October 2010

Keywords:
Ethyl acetate
Ethanol
Dehydrogenation
Bioethanol

ABSTRACT

Ethanol produced from cellulosic residues will be in large supply all over the world in the next decades. Undoubtedly, bioethanol will be used as a gasoline substitute or additive. Taking its future large availability into account, its use as feedstock for the chemical industry can also be foreseen. The ethyl acetate one-pot synthesis from ethanol is a good example of this new industry. This contribution aims to describe the dehydrogenative route of the ethyl acetate one-pot synthesis and also the role of the support using physical mixtures comprised of a dehydrogenation catalyst and four different oxides. The solids were characterized employing TPD of ethanol, CO_2 and acetaldehyde and also pyridine adsorption. It was verified that acetaldehyde synthesized on the dehydrogenation catalyst migrates towards the oxide and reacts with the ethoxide species which are generated by the oxide basic sites. The resulting hemiacetal is dehydrogenated and the ethyl acetate obtained is desorbed. Oxides with strong basic sites generate the most active and selective systems for the ethyl acetate synthesis.

1. Introduction

The production of ethanol from cellulosic residues will generate a large supply of bioethanol all over the world in the next decades, which will be used as a gasoline substitute or additive. Taking this future large availability of bioethanol into account, the use of ethanol as feedstock for the chemical industry can also be foreseen.

Ethyl acetate has been largely employed as a solvent in paints, coatings, inks and adhesives. It replaces aromatic compounds which cause serious damage to human beings and the environment [1]. The one-pot synthesis of ethyl acetate from ethanol, which has been suggested by some authors, is an interesting example of this new industry. Two different routes have been proposed: the oxidative [2] and the dehydrogenative routes [3–5]. The last one is already being industrially exploited using Cu/Cr_2O_3 as catalyst and ethanol generated from the Fischer–Tropsch process.

Studying the dehydrogenative route and using $Cu/ZnO/Al_2O_3/ZrO_2$ as catalyst, Inui et al. [6] suggested that ethanol is first dehydrogenated to acetaldehyde and then reacts with another ethanol or ethoxide species to form a hemiacetal, which is then dehydrogenated to ethyl acetate. These authors suggested that acetaldehyde is adsorbed on an acid site, whereas the ethoxide species are generated by basic sites.

Not long ago, our group studied the synthesis of ethyl acetate from ethanol working with physical mixtures ($Cu/ZnO/Al_2O_3 + ZrO_2$) and suggested that: firstly, acetaldehyde is generated on the $Cu/ZnO/Al_2O_3$ catalyst; then it migrates towards the oxide (spillover) and reacts with ethanol or ethoxide species generating hemiacetal, which is then dehydrogenated producing ethyl acetate [7].

Some studies show that the support can play a very important role in this synthesis. Iwasa and Takezawa [8] using Cu/ZrO_2 and Cu/SiO_2 catalysts suggested that the condensation reaction between ethanol and acetaldehyde occurs on the Cu/ZrO_2 support, whereas for the Cu/SiO_2, it occurs on the copper surface. Sanchez et al. [5] using palladium (1 wt.% Pd) supported catalyst showed that the support changes the catalytic behavior. They verified that palladium supported on SnO_2 or ZnO is much more selective to ethyl acetate than on Al_2O_3 or SiO_2.

The main physico-chemical properties which determine the behavior of the oxides in the condensation reaction still remain unknown. It is also not clear which species, ethanol or ethoxide, are involved in this reaction. Recently, it was suggested that the spillover phenomenon might occur during this synthesis [7]. However, more experimental observations are needed in order to prove it.

Thus, this contribution aims to describe the dehydrogenative route of the ethyl acetate one-pot synthesis and also the role of the

* Corresponding author. Tel.: +55 21231165.
E-mail address: lucia.appel@int.gov.br (L.G. Appel).

1381-1169
doi:10.1016/j.molcata.2010.10.019

support using physical mixtures consisting of a dehydrogenation catalyst and four different oxides.

2. Experimental

2.1. Catalyst and oxides preparation

A commercial $Cu/ZnO/Al_2O_3$ was used as the dehydrogenation catalyst. It was named CZA. The oxides employed in the physical mixtures were ZrO_2 (monoclinic), CeO_2, Al_2O_3 and SiO_2. The ZrO_2 and the Al_2O_3 were commercial samples supplied by Norpro and the SiO_2 sample by Davison. The CeO_2 sample was synthesized according to Hori et al. [9] procedure. An aqueous solution of $(NH_4)_2(Ce(NO_3)_6)$ (0.2 mol L^{-1}) was abruptly added to a NH_4OH solution. The precipitate formed was filtered and washed with distilled water until the pH was equal to 7. The solid obtained was calcined at 773 K for 1 h at 10 K min^{-1}.

2.2. Samples characterization

Pyridine thermodesorption experiments followed by IR spectroscopy were conducted to probe the acid properties of the oxides using a Nicolet Magna spectrophotometer. The spectra were recorded using thin (20 mg) self-supporting wafers. The samples were pretreated at 673 K for 2 h under high vacuum, submitted to air pulses at the same temperature for 1 h and exposed again to high vacuum for 30 min. Pyridine was adsorbed at room temperature for 30 min at 2 Torr. The spectra were collected after desorption at 298 and 423 K for 1 h under high vacuum. The values of the acid density were obtained considering the absorption around 1445 cm^{-1}. The FTIR results were normalized by the wafers mass.

The temperature-programmed desorption (TPD) of ethanol, acetaldehyde and CO_2 experiments were carried out using a micro reactor system coupled to a QMS200 Balzers mass quadrupole spectrometer. For all these experiments the mass samples were 100, 100, 200 mg for CZA, ZrO_2 and CZA + ZrO_2 (1/1), respectively. Before the TPD of ethanol and acetaldehyde, the samples were pretreated under He flow (20 mL min^{-1}) at 393 K for 1 h. After that, the catalysts were reduced at 523 K under H_2/He (10%, v/v) flow (60 mL min^{-1}) for 1 h. In the case of the TPD of CO_2 experiments, the samples pretreatment was the following: 773 K (10 K min^{-1}) under O_2/He (8%, v/v) flow (40 mL min^{-1}) for 1 h. After that, the samples were reduced according to the procedure described above.

2.2.1. TPD of ethanol

The adsorption of ethanol was conducted at room temperature for 1 h. Ethanol vapors were generated by passing He (40 mL min^{-1}) through a saturator at 303 K. The ethanol TPD measurements were carried out heating the samples at 20 K min^{-1} up to 773 K, under He flow (40 mL min^{-1}). The products were continuously monitored by a mass spectrometer. The fragments 31 and 44 were assigned to ethanol and acetaldehyde, respectively. Indeed, the main fragment of acetaldehyde (m/z = 29) includes contributions of ethanol and ethyl acetate, thus the second most intense fragment (m/z = 44) was chosen.

2.2.2. TPD of acetaldehyde

Acetaldehyde was adsorbed at room temperature employing a mixture of acetaldehyde and N_2 (4%, v/v) for 1 h which was fed at 20 mL min^{-1}. The acetaldehyde desorption conditions were the same ones used for ethanol TPD. During the desorption procedure the acetaldehyde fragment m/z = 44 was monitored.

2.2.3. TPD of CO_2

Finally, the CO_2 adsorption was conducted at room temperature for 1 h (12 mL min^{-1}). The desorption conditions were the same ones used for the temperature-programmed desorption of ethanol and acetaldehyde described above. The CO_2 fragment (m/z = 44) was continuously monitored as well. The TPD profiles were decomposed in Gaussian curves in order to quantify the weak, medium and strong basic sites. The basic sites which are assigned as weak are related to a curve which shows a maximum at a temperature lower than 400 K, the ones between 400 and 580 K, medium; and finally, the ones above 580 K, strong basic sites [10].

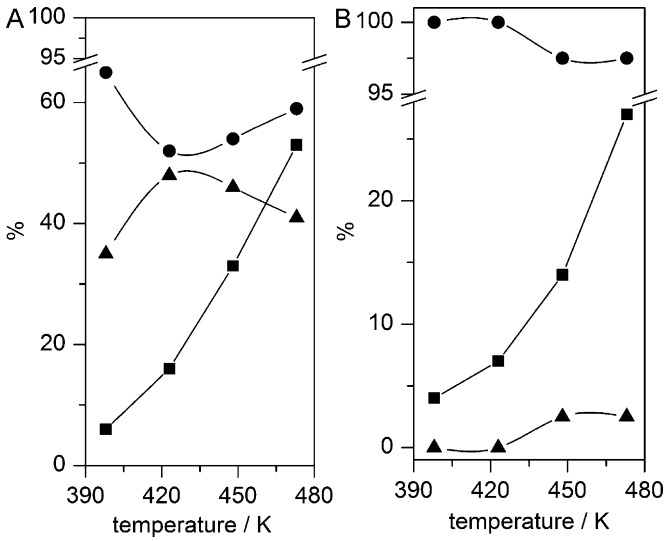

Fig. 1. (A) Ethanol conversion and selectivities over CZA + ZrO_2 physical mixture versus temperature. The symbols ■, ●, ▲ refer to ethanol conversion and selectivities towards acetaldehyde and ethyl acetate, respectively. The flow rate, ethanol concentration in N_2 stream, mass of the physical mixture and ratio among the physical mixture components were 20 mL min^{-1}, 12% and 200 mg, 1/1, respectively. (B) Ethanol conversion and selectivities over CZA + SiO_2 physical mixture versus temperature. The symbols ■, ●, ▲ refer to ethanol conversion and selectivities towards acetaldehyde and ethyl acetate, respectively. The flow rate, ethanol concentration in N_2 stream, mass of the physical mixture and ratio among the physical mixture components were 20 mL min^{-1}, 12% and 200 mg, 1/1, respectively.

2.3. Ethyl acetate synthesis

The catalytic tests were performed using a conventional system with a fixed bed reactor at atmospheric pressure and monitored by on-line gas chromatography. A 12% ethanol/N_2 (vol.%) mixture was fed at 20 mL min^{-1} on a catalyst mass of 100 mg. Ethanol vapors were generated by passing N_2 through a saturator at 303 K. The catalysts were reduced at 523 K for 1 h under H_2/N_2 (17%, v/v). The weight ratio employed among the physical mixture components was catalyst/oxide = 1. Aiming to analyze the catalytic behavior of the dehydrogenation catalyst (CZA), the oxides were replaced by quartz in some catalytic tests. Some experiments were also carried out using a downflow double bed reactor. The upper layer was composed of CZA and the oxides were in the second layer. In the case of the double bed reactor, the experimental conditions employed were the same described above. The ethanol consumption rates were calculated under differential conditions (ethanol conversion <10%).

3. Results and discussion

The ethanol conversion and the selectivities to ethyl acetate and acetaldehyde versus the reaction temperature for CZA ($Cu/ZnO/Al_2O_3$) + ZrO_2 and CZA + SiO_2 physical mixtures are shown in Fig. 1A and B, respectively. Fig. 1A shows that as the temperature of the reaction increases, so does the conversion. The selectivity towards ethyl acetate also increases reaching a maximum around

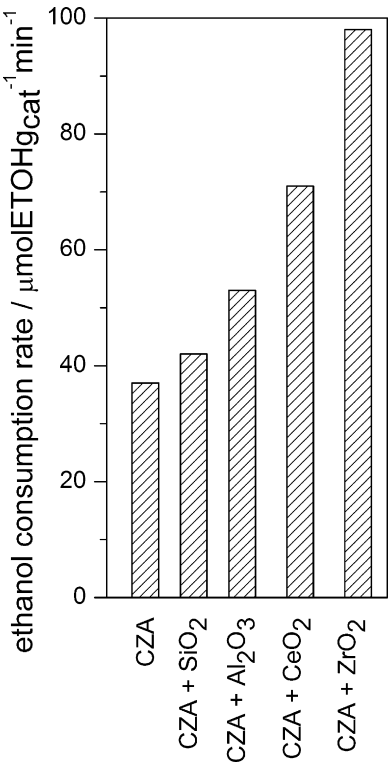

Fig. 2. Ethanol consumption rate of the physical mixtures at 423 K. The experimental conditions are the same ones mentioned in Fig. 1.

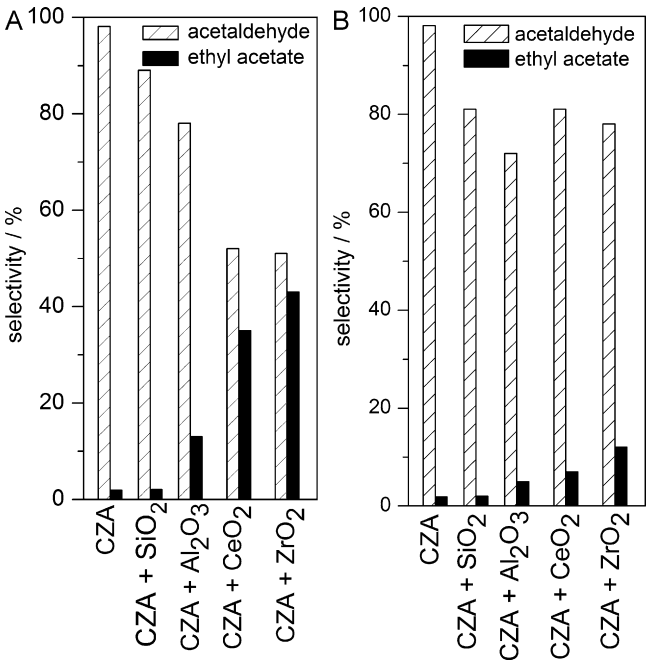

Fig. 3. (A) Selectivities of the physical mixtures towards acetaldehyde and ethyl acetate at 30% of ethanol conversion. The reaction temperatures were 448 K for ZrO_2 and CeO_2 and 473 K for SiO_2 and Al_2O_3. The other experimental conditions are the same ones mentioned in Fig. 1. (B) Selectivities of the double bed reactor towards acetaldehyde and ethyl acetate, at 30% of ethanol conversion and 473 K. The other experimental conditions are the same ones mentioned in Fig. 1.

423 K, after which it decreases. This figure also shows that as the selectivity to ethyl acetate increases, the selectivity to acetaldehyde decreases, and vice-versa. In the case of CZA + SiO_2, the main product obtained is acetaldehyde. Ethanol conversion and selectivity to ethyl acetate values are lower when compared with the ZrO_2 results. These observations agree with the ones reported by Iwasa and Takezawa [8] and also show that the support plays an important role in this synthesis.

Fig. 2 displays the results of the ethanol consumption rate of CZA and the physical mixtures composed of CZA and four distinct oxides (ZrO_2, CeO_2, Al_2O_3 and SiO_2). These data were obtained at 423 K. As it can be verified, CZA and CZA + SiO_2 show the lowest rates and the physical mixture with ZrO_2, the highest. The physical mixtures comprised of Al_2O_3 and CeO_2 generated intermediary values of the ethanol consumption rate.

Fig. 3A shows the selectivities to ethyl acetate and acetaldehyde employing CZA and the physical mixtures at similar conversion (~30%). These results show that the selectivities towards ethyl acetate and acetaldehyde change according to the composition of the physical mixture. On the one hand, the physical mixture comprised of SiO_2 shows the lowest selectivity to ethyl acetate and the highest one to acetaldehyde. On the other hand, the physical mixture with ZrO_2 displays the highest selectivity towards ethyl acetate and the lowest to acetaldehyde. Intermediary values of the selectivity towards acetaldehyde and ethyl acetate were generated by physical mixtures comprised of Al_2O_3 and CeO_2.

Comparing Figs. 2 and 3A, it can be verified that the catalytic systems which show high selectivity to ethyl acetate also show a high ethanol consumption rate. It can also be observed that CZA shows the lowest rate and that it generates mostly acetaldehyde. Taking the thermodynamic data related to the dehydrogenation of ethanol to acetaldehyde into account [11], it can be inferred that when only CZA is employed this reaction is near the thermodynamic equilibrium. These results suggest that the condensation reaction, i.e., the ethyl acetate synthesis shifts the equilibrium of the dehydrogenation reaction. All these results also depict that the condensation reaction occurs on the surfaces of the oxides (Al_2O_3, CeO_2 and ZrO_2).

The selectivities to ethyl acetate and acetaldehyde at similar conversion (30%) employing double bed reactors are depicted in Fig. 3B. Comparing these results with the ones of the physical mixtures, it can be verified that the selectivities to ethyl acetate are much lower and to acetaldehyde higher. However, the same ethyl acetate selectivity trends related to the oxides behavior can be observed for both reactors. The ethanol consumption rates of the double bed reactors are low and similar to the ones observed for CZA. Hence, taking into account that the first bed was comprised of CZA and the second of oxides and that the condensation reaction occurs at very low rate, these results suggest that the readsorption of acetaldehyde or/and ethanol on the oxides occurs at very low rate. Therefore, it can be proposed that there is a synergy between CZA and the oxides when physical mixtures were employed, which is more intense in the case of CeO_2 and ZrO_2.

Working with the same catalytic system and experimental conditions, our group recently published [7] that doubling or even quadrupling the amount of ZrO_2 in the physical mixtures, only a small decrease of the ethanol conversion and of the ethyl acetate selectivity was observed. These results and the ones of the double bed reactor described above suggest that the interface between the catalyst and the oxides is extremely relevant for the ethyl acetate synthesis under these conditions. Moreover, readsorption of acetaldehyde or/and ethanol on the oxides seems not to play an important role in the ethyl acetate synthesis.

Aiming to better describe this phenomenon, TPD of ethanol and acetaldehyde were carried out. Fig. 4A and B shows the TPD of ethanol on ZrO_2, CZA and CZA + ZrO_2 physical mixture. Fig. 4A is related to ethanol (fragment $m/z = 31$). As it can be observed, ethanol can be adsorbed on ZrO_2, CZA and also CZA + ZrO_2 physical mixture. One main peak at 476, 411 and 440 K was observed for the three samples, respectively. These profiles also show desorptions at higher temperatures.

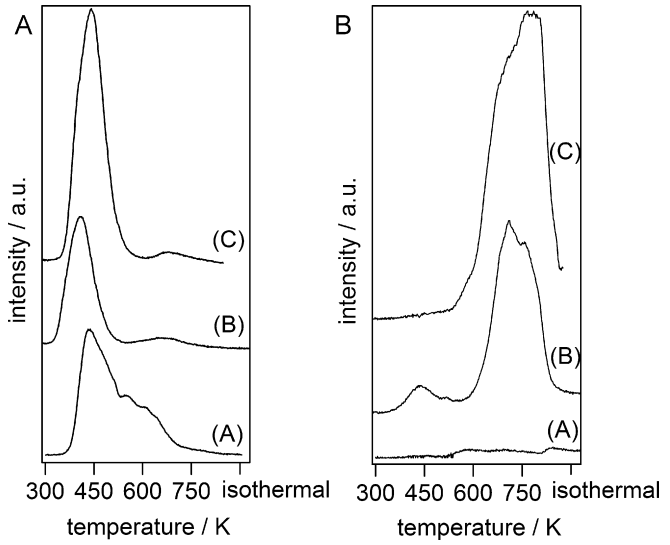

Fig. 4. (A) TPD spectrum of ethanol ($m/z = 31$) over ZrO_2 (A), $Cu/ZnO/Al_2O_3$ (B), $Cu/ZnO/Al_2O_3 + ZrO_2$ (C). (B) TPD spectrum of ethanol ($m/z = 44$) over ZrO_2 (A), $Cu/ZnO/Al_2O_3$ (B), $Cu/ZnO/Al_2O_3 + ZrO_2$ (C).

Fig. 4B depicts the desorption of acetaldehyde which is synthesized during the TPD of ethanol employing ZrO_2, CZA and the physical mixture of these two solids. As it can be inferred, acetaldehyde is not synthesized when only ZrO_2 is used.

Therefore, these results show that during the catalytic test with the physical mixtures, ethanol can be adsorbed on the oxide whereas the aldehyde might spillover from the copper catalyst towards the oxide or be transported by vapor phase and readsorbed on the oxide surface. According to Pajonk [12], the contact between the donor and the acceptor of the mobile compound is an important parameter of the spillover phenomenon. The more intimate contact, the greater the spillover effect. Taking the data of the double bed and also our previous results into account [7], the spillover phenomena seems to be more relevant. After that, acetaldehyde reacts with ethanol or ethoxide species in order to generate ethyl acetate.

Fig. 5 shows the TPD of acetaldehyde (fragment $m/z = 44$) employing m-ZrO_2, CZA and CZA + ZrO_2 physical mixture. Three sites of acetaldehyde desorption on ZrO_2 at 377, 663, 773 K can be observed. The copper catalyst (CZA) also shows three different peaks which are at 364, 573, 744 K. This catalyst is able to adsorb much more species than ZrO_2. These species need less energy to be desorbed than the ones adsorbed on ZrO_2. The TPD profile of the physical mixture shows the main peak at a much higher temperature than the main one of CZA. On the other hand, the TPD profile of the physical mixture is similar to the one of ZrO_2, although the amount of acetaldehyde desorbed is much higher. This result suggests that acetaldehyde adsorbed on CZA might spillover to ZrO_2 and then desorbs. Therefore, it can be suggested that the spillover rate is higher than the acetaldehyde desorption from CZA surface. One can also suggest that acetaldehyde readsorption can occur during TPD. However, taking our results into account the rate of acetaldehyde readsorption on the ZrO_2 seems to be low.

Taking the TPD spectra of acetaldehyde (Fig. 5) into account, the results of the double bed reactor and also our previous observations [7], it can be proposed that acetaldehyde is generated by ethanol dehydrogenation on the CZA surface. After that, it spillovers towards the oxide and reacts with ethanol or ethoxide, generating the hemiacetal, which is then dehydrogenated to ethyl acetate. One can suggest that this dehydrogenation might also occur on the CZA surface. However, we did not observe the hemiacetal. According to Inui et al. [6], this intermediate could exist as unstable adsorbed species. Therefore, its dehydrogenation should occur promptly on the oxide.

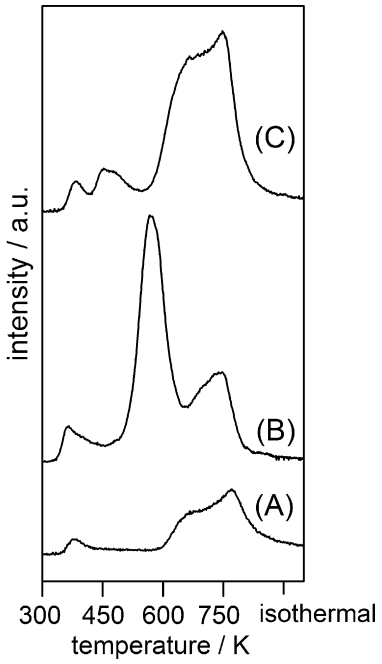

Fig. 5. TPD spectrum of acetaldehyde ($m/z = 44$) over ZrO_2 (A), $Cu/ZnO/Al_2O_3$ (B), $Cu/ZnO/Al_2O_3 + ZrO_2$ (C).

The acid and basic properties of the oxides were analyzed in order to understand the catalytic behavior of these solids when employed in the physical mixtures.

The pyridine adsorptions on ZrO_2, Al_2O_3, CeO_2 and SiO_2 were analyzed by FTIR. All spectra obtained after pyridine adsorption at 298 K and desorption at 298 K and 423 K display absorptions around 1610 and 1445 cm^{-1}. The ZrO_2, Al_2O_3 and CeO_2 oxides also show absorptions at 1490 cm^{-1}. According to the literature, all these bands can be assigned to Lewis acid sites [13]. Table 1 depicts that Al_2O_3 showed the highest Lewis acid sites density followed by ZrO_2, CeO_2 and SiO_2 at 298 K and also at 423 K.

Busca [14] reported that ring vibration mode frequencies change according to the interaction of pyridine with Lewis acid sites, being the 8a mode the most sensitive. This mode is located at 1583 cm^{-1} for liquid-like (Van der Waals) physically adsorbed pyridine [15]. Depending on the acid strength of the Lewis centers, the pyridine adsorption band shifts upward accordingly. The higher the acid strength, the higher the shift. The shifts of the oxides which were analyzed are depicted in Table 1. Taking these values into account, the acid strength order is $Al_2O_3 > ZrO_2 > CeO_2 > SiO_2$, which is the same one observed for the density of the acid sites (Table 1). The changes of the acid sites density values when the desorption temperature increases from 298 K to 423 K is in line with the results shown above. As it can be observed (Table 1), Al_2O_3 shows the largest shift amongst all the oxides, i.e., Al_2O_3 depicts the strongest acid sites. It also shows the highest acid sites density. However, its physical mixture does not show the highest activity, neither the

Table 1
Optical densities of the band at 1445 cm^{-1} obtained by pyridine adsorption at 298 K (L_1) and 423 K (L_2) and the shift values of the 8a mode (δ).

Oxide	L_1 (aug^{-1})	L_2 (aug^{-1})	δ (cm^{-1})
m-ZrO_2	120	43	22
Al_2O_3	243	100	33
SiO_2	66	0	15
CeO_2	87	28	19

Table 2
Specific surface area (*A*), density of weak basic sites (*W*), density of medium basic sites (*M*), density of strong basic sites (*S*) and density of basic sites (*T*).

Oxides	A ($m^2\,g^{-1}$)	W ($\mu mol\,g^{-1}$)	M ($\mu mol\,g^{-1}$)	S ($\mu mol\,g^{-1}$)	T ($\mu mol\,g^{-1}$)
SiO_2	261	–	–	–	–
Al_2O_3	294	70	85	–	155
CeO_2	86	74	56	33	163
ZrO_2	110	58	137	35	230

highest selectivity to ethyl acetate. As it was already mentioned, the condensation reaction occurs on acid and basic sites [6]. However, this result suggests that the acid properties are not relevant to describe the oxides behavior.

The results related to the TPD of CO_2 of the oxides are depicted in Fig. 6 and Table 2. As it can be verified, these oxides show different profiles regarding their interaction with CO_2.

The SiO_2 sample almost does not interact with CO_2. It is interesting to verify that the SiO_2 physical mixture is the less active system and also the less selective to ethyl acetate, suggesting that the basic properties might be relevant. As it can be observed in Table 2, alumina shows only weak and medium basic sites.

The ZrO_2 and CeO_2 samples show weak, medium and strong basic sites (Table 2). Their profile (TPD) is almost similar. However, ZrO_2 shows much more medium-strength basic sites.

Alumina (155 $\mu mol\,g^{-1}$) and ceria (163 $\mu mol\,g^{-1}$) show almost the same number of basic sites (Table 2). However, the latter shows a much higher selectivity towards ethyl acetate than alumina (Fig. 3A). On the other hand, zirconia shows a higher number of basic sites (230 $\mu mol\,g^{-1}$) than ceria. Their selectivities to ethyl acetate are not very different though (Fig. 3). Comparing the density of the strong basic sites on zirconia and ceria and their catalytic behavior, one can infer that these sites might play an important role in the ethyl acetate synthesis.

As mentioned in Section 2, only the reduction procedure was employed before the catalytic test. Therefore, it was necessary to quantify the amount of basic sites available for the reaction or, in other words, evaluate if the surface was already contaminated by carbonate species before the reaction. Thus, ZrO_2 sample was submitted to reduction procedure and, after that, a TPD without CO_2 adsorption was carried out, employing the same experimental conditions described above. Only a small amount of strong basic sites were observed (less than 10% of the strong basic sites analyzed by the TPD of CO_2, Table 2). Thus, it can be inferred that the reduction process is able to eliminate almost all the carbonate residues on the zirconia sample. We suggest that the same occurs for the other oxides.

Fig. 7 shows the correlation between the total number of basic sites and the selectivity to ethyl acetate at similar conversion (30%). It can be verified that, as the number of basic sites increases, the selectivity increases as well. In order to demonstrate the role of the strong basic sites, the density of these sites was multiplied by 11 (this value was obtained empirically) and added to the density of weak and medium basic sites. Fig. 7 depicts a linear correlation between the modified density of the basic sites and the selectivity to ethyl acetate. Therefore, strong basic sites are much more relevant than medium and weak ones for the ethyl acetate synthesis.

As mentioned above, the higher the selectivity to ethyl acetate, the higher the ethanol consumption rate (Figs. 2 and 3A). Thus, a correlation between density of the basic sites and the rate of ethanol consumption can also be suggested. According to Inui et al. [6], basic sites are associated to the generation of ethoxide species. Therefore, the results obtained suggest that the ethoxide formation is a very important step of the ethyl acetate synthesis and might be the rate limiting step under these conditions.

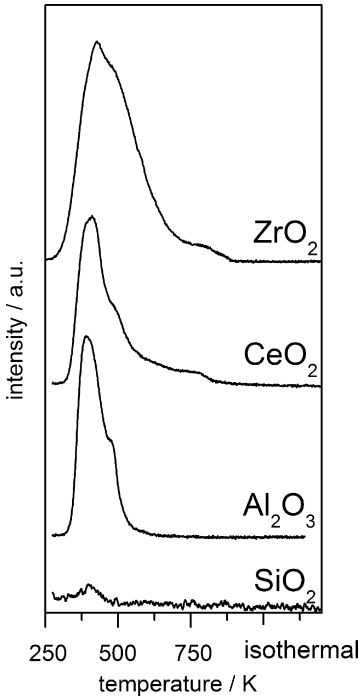

Fig. 6. TPD spectra of CO_2 ($m/z = 44$).

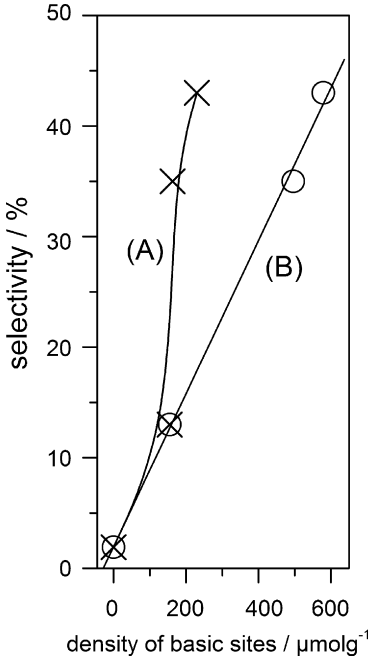

Fig. 7. Ethyl acetate selectivity versus the total amount of basic sites (A) and versus the total amount of basic sites multiplying the strong basic sites by 11 (weak + medium + strong × 11) (B).

4. Conclusion

These results show that acetaldehyde is generated by ethanol dehydrogenation on CZA. After that, it spillovers towards the oxide and reacts with ethoxide species, which are generated by the basic sites of this oxide. Then, the hemiacetal obtained is dehydrogenated and the ethyl acetate is desorbed. These results also show that the condensation reaction increases the rate of ethanol consumption. The oxides that have strong basic sites generated the most active and selective systems. Therefore, the ethoxide formation might be the rate limiting step. As it is well known, spillover can occur during many different reactions [16]. This work also suggests that physical mixtures can be an interesting tool in order to identify this phenomenon.

References

[1] R. Sakamuri, in: R.E. Kirk, D.F. Othmer (Eds.), Kirk–Othmer Encyclopedia of Chemical Technology, vol. 10, 5th ed., John Wiley & Sons, Wiley Interscience, New Jersey, 2004, pp. 497–513.
[2] A.B. Gaspar, A.M.L. Esteves, F.M.T. Mendes, F.G. Barbosa, L.G. Appel, Appl. Catal. A 363 (2009) 109–114.
[3] K. Inui, T. Kurabayashi, S. Sato, J. Catal. 212 (2002) 207–215.
[4] S.W. Colley, J. Tabatabaei, K.C. Waugh, M.A. Wood, J. Catal. 236 (2005) 21–33.
[5] A.B. Sanchez, N. Homs, J.L.G. Fierro, P.R. de la Piscina, Catal. Today 107–108 (2005) 431–435.
[6] K. Inui, T. Kurabayashi, S. Sato, N. Ichikawa, J. Mol. Catal. A: Chem. 216 (2004) 147–156.
[7] A.B. Gaspar, F.G. Barbosa, S. Letichevsky, L.G. Appel, Appl. Catal. A 380 (2010) 113–117.
[8] N. Iwasa, N. Takezawa, Bull. Chem. Soc. Jpn. 64 (1991) 2619–2623.
[9] C.E. Hori, H. Permana, K.Y.S. Ng, A. Brenner, K. More, K.M. Rahmoeller, D.N. Belton, Appl. Catal. B 16 (1998) 105–117.
[10] Z.Y. Ma, C. Yang, W. Wei, W.H. Li, Y.H. Sun, J. Mol. Catal. A: Chem. 227 (2005) 119–124.
[11] W. Dai, L. Ren, in: G. Ertl, H. Knozinger, F. Schuth, J. Weitkamp (Eds.), Handbook of Heterogeneous Catalysis, vol. 7, 2nd ed., Wiley-VCH, Weinheim, 2008, pp. 3256–3265 (Chapter 14).
[12] G.M. Pajonk, in: G. Ertl, H. Knozinger, F. Schuth, J. Weitkamp (Eds.), Handbook of Heterogeneous Catalysis, vol. 3, 1st ed., Wiley-VCH, Weinheim, 1997, pp. 1064–1077.
[13] H.G. Karge, in: G. Ertl, H. Knozinger, F. Schuth, J. Weitkamp (Eds.), Handbook of Heterogeneous Catalysis, vol. 2, 2nd ed., Wiley-VCH, Weinheim, 2008, pp. 1096–1122 (Chapter 3).
[14] G. Busca, Catal. Today 41 (1998) 191–206.
[15] C. Binet, M. Daturi, J.C. Lavalley, Catal. Today 50 (1999) 207–225.
[16] F. Rößner, in: G. Ertl, H. Knozinger, F. Schuth, J. Weitkamp (Eds.), Handbook of Heterogeneous Catalysis, vol. 3, 2nd ed., Wiley-VCH, Weinheim, 2008, pp. 1574–1585 (Chapter 5).